RSC Advances

PAPER

View Article Online
View Journal | View Issue

Cite this: *RSC Adv.*, 2016, **6**, 93205

Palladium nanoparticles stabilised by cinchona-based alkaloids in glycerol: efficient catalysts for surface assisted processes†

A. Reina,[a] C. Pradel,[a] E. Martin,[b] E. Teuma[a] and M. Gómez*[a]

Received 29th July 2016
Accepted 20th September 2016

DOI: 10.1039/c6ra19230k

www.rsc.org/advances

Palladium nanoparticles (PdNPs) were synthesised and fully characterised, both in solution and the solid state, using naturally-occurring cinchona-based alkaloids in neat glycerol. These nano-systems were stable under reaction conditions, finding applications in hydrogenation and hydrodehalogenation processes, as a result of their surface-like behaviour. Their reactivity was improved in relation to that involving PdNPs stabilised by phosphines and also by Pd/C as a heterogenous catalyst, mainly in terms of recyclability. In particular, the colloidal palladium catalyst stabilised by quinidine was highly efficient to promote the hydrodechlorination of aromatic compounds under low dihydrogen pressure. These original catalysts found applications in the synthesis of secondary and tertiary amines including *N*-substituted anilines, by means of one-pot tandem Pd-catalysed methodologies under smooth conditions. In all of these processes, glycerol performed a crucial function as a liquid support for the immobilisation of nanoparticle-based catalysts, allowing both the stabilisation of the nano-catalysts and easy recycling of the catalytic phase.

Introduction

Palladium represents one of the most efficient and versatile metal-based catalysts, finding applications in a large variety of processes (couplings, carbonylations, hydrogenations…) under different material states, including molecular complexes, nanoparticles and extended surfaces,[1] and permitting immobilisation on both solid supports[2] and liquid phases.[3] This structural variety leads to different kinds of activations, a reason for which palladium is the most used metal in organic synthesis.[4]

In the last decades, huge efforts have been done in the preparation of metal nanoparticles and in particular in palladium nanoparticles (PdNPs), controlling their size, composition and morphology, parameters able to directly impact on the further catalytic reactivity.[5] From a mechanistic point of view, some studies seem to prove that nano-sized starting catalytic precursors can act as a reservoir of small clusters or atoms, probably operating under homogeneous regime. But catalytic processes involving defined organometallic compounds, such as cyclometallated complexes, also lead to the formation of PdNPs mostly at high temperatures, which can give rise to a surface reactivity.[6] The various plausible scenarios can be adjust modifying reaction conditions, nature of stabilisers, solvent… principally when PdNPs are homogeneously dispersed in a liquid phase. Contrary to common organic solvents, structurally organised ones (for instance, imidazolium-based ionic liquids[7] or polyols[8]) by intermolecular hydrogen bonds or π–π stacking assemblies, can make easy the stabilisation of nanoparticles, avoiding their agglomeration and in consequence favouring a heterogeneous reactivity.[9] However because of the relative weak interactions between solvents and metal surfaces, the addition of stabilisers other than solvents is in general required for both inducing activity and/or selectivity in the catalytic processes and stabilising the nano-sized state.[10]

In a sustainable frame, the design of eco-friendly catalysts represents a major concern. Our experience in the development of catalytic processes in glycerol involving metal nanoparticles,[11,12] in particular those using PdNPs stabilised by phosphines,[12] led us to work with stabilisers coming from the biomass, such as cinchona-based alkaloids, well-known for their use in stereoselective reactions, mainly in enantioselective hydrogenations where nanoparticles are supported in different kinds of materials.[13] In contrast to the strong interactions between P-donor ligands and metal surface, primarily by dative σ/π Pd–P interactions, cinchona ligands can interact with the surface through N-quinoline atom or by π interaction through the aromatic ring,[14] disfavouring the formation of defined

[a]*Laboratoire Hétérochimie Fondamentale et Appliquée (LHFA), Université de Toulouse, UPS, CNRS UMR 5069, 118, route de Narbonne, 31062 Toulouse cedex 9, France. E-mail: gomez@chimie.ups-tlse.fr*

[b]*Departamento de Química Inorgánica, Facultad de Química, Universidad Nacional Autónoma de México, Av. Universidad 3000, 04510 México DF, Mexico*

† Electronic supplementary information (ESI) available: General experimental part, Tables S1 and S2, Fig. S1–S19, Schemes S1–S4 and ^{1}H and ^{13}C NMR spectra of the products obtained in the catalytic reactions are included. See DOI: 10.1039/c6ra19230k

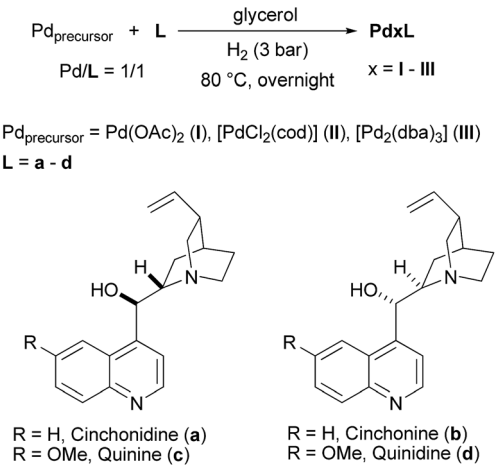

Scheme 1 Synthesis of palladium nanoparticles PdxL in glycerol using cinchona-based alkaloids (**a–d**) as stabilisers ([Pd] = 10^{-2} mol L^{-1}).

coordination complexes, and in consequence, privileging the stabilisation of nanoparticles more than molecular species.

In this context, we decided to explore the catalytic reactivity of palladium nanoparticles prepared in glycerol in the presence of naturally-occurring cinchona-based alkaloids, in particular the optically pure stereoisomers cinchonidine, cinchonine, quinine and quinidine (Scheme 1). We chose hydrogenations and hydrodehalogenations because of their presumed heterogeneous pathway. To the best of our knowledge, no precedents in the literature using palladium nanoparticles stabilised by cinchona ligands as colloidal catalysts have been previously reported.[15]

Experimental

Synthesis of palladium nanoparticles in glycerol

0.05 mmol of palladium precursor (11.2 mg for $Pd(OAc)_2$; 14.1 mg for $[PdCl_2(cod)]$; 22.8 mg $[Pd_2(dba)_3]$) and 0.05 mmol of ligand (14.7 mg for cinchonidine (**a**) and cinchonine (**b**); 16 mg for quinine (**c**) and quinidine (**d**); 28.4 mg for TPPTS) were dissolved in 5 mL of glycerol and stirred under argon in a Fisher–Porter bottle at room temperature until complete dissolution. The system was then pressurized under 3 bar of dihydrogen and stirred at 80 °C for 18 h. A black colloidal solution was then obtained.

Isolation of palladium nanoparticles from the glycerol solution

After synthesis, PdNPs in glycerol were transferred to a centrifugation tube and 2 mL of ethanol were added. Centrifugation was carried out at 600 rpm for 5 h and then the solution was separated by decantation. This process was repeated 3 times until complete removal of glycerol. The remaining black powder was then dried under vacuum at 80 °C overnight. Elementary analysis (palladium load determined by ICP-AES): **PdIa**: Pd 26.5%, C 57%, N 7%, H 5.5%; **PdId**: Pd 25%, C 56%, N 6.5%, H 5.6%.

Ligand exchange reaction at the surface of palladium nanoparticles

In a Schlenk flask under argon, 1 equivalent of dodecanethiol (0.05 mmol; 10.12 mg) were added to 1 mL of colloidal solution (**PdIa** or **PdId**) and stirred for 24 h. Ligands **a** or **d** were extracted form the glycerol phase with dichloromethane (10 × 3 mL); dichloromethane was removed under vacuum. The mixture extracted was analysed by ^{1}H NMR.

Hydride titration of palladium nanoparticles

Isolated **PdIa** or **PdId** (0.02 mmol, 2.1 mg) were added to a Young NMR tube under argon at room temperature containing 0.6 mL of THF-d_8 and maleic anhydride (0.01 mmol, 1 mg) in the presence of an external standard (0.01 mmol – 113 mg of cyclooctane). The corresponding mixtures were monitored by ^{1}H NMR.

General procedure for Pd-catalysed hydrogenation in glycerol

In a Fisher–Porter bottle (from 1 to 5 bar) or an autoclave (5 to 20 bar), the appropriate substrate (1 mmol for 1 mol% of catalyst; 5 mmol for 0.5 mol% or 10 mmol for 0.1 mol%) was added to 1 mL of preformed nanoparticles in glycerol under argon. The reaction mixture was put under vacuum and then pressurised with H_2 at the convenient pressure, heated up to the desired temperature, stirred for the appropriate time and then cooled down to room temperature. Organic products were extracted from glycerol with dichloromethane (5 × 3 mL) dichloromethane was removed under vacuum. All the products were previously reported and identification was done by comparison of their GC-MS data and ^{1}H and ^{13}C NMR spectra with the reported data.

General procedure for Pd-catalysed hydrodehalogenation in glycerol

In a Fisher–Porter bottle (from 1 to 5 bar H_2) or an autoclave (5 to 20 bar H_2), the appropriate aryl-halide (1 mmol for 1 mol% of catalyst; 5 mmol for 0.5 mol%; 10 mmol for 0.1 mol%) was added to 1 mL of preformed nanoparticles in glycerol under argon (total amount of palladium: 0.01 mmol). If necessary, 1.2 equivalents of KOH (66 mg) were also added. The reaction mixture was put under vacuum and then pressurised with H_2 at the convenient pressure, heated up to the desired temperature, stirred for the appropriate time and then cooled down to room temperature. Organic products were extracted from glycerol with dichloromethane (5 × 3 mL); dichloromethane was removed under vacuum. All the products were previously reported and identification was done by comparison of their GC-MS data and ^{1}H and ^{13}C NMR spectra with the reported data.

General procedure for Pd-catalysed synthesis of secondary and tertiary amines

In a Fisher–Porter bottle the appropriate primary or secondary amine (1 mmol) and aldehyde (1 mmol) were added to 1 mL of preformed nanoparticles in glycerol under argon (total amount of palladium: 0.01 mmol). The reaction mixture was put under

vacuum and then pressurised with H_2 at the convenient pressure, heated up to the desired temperature, stirred for the appropriate time and then cooled down to room temperature. Organic products were extracted from glycerol with dichloromethane (5 × 3 mL); dichloromethane was removed under vacuum. All the products were previously reported and identification was done by comparison of their GC-MS data and ^{1}H and ^{13}C NMR spectra with the reported data.

General procedure for Pd-catalysed synthesis of N-substituted anilines

In a Fisher–Porter bottle nitrobenzene (1 mmol) and the appropriated aldehyde (1 mmol) were added to 1 mL of preformed nanoparticles in glycerol under argon (total amount of palladium: 0.01 mmol). The reaction mixture was put under vacuum and then pressurised with H_2 at the convenient pressure, heated up to the desired temperature, stirred for the appropriate time and then cooled down to room temperature. Organic products were extracted from glycerol with dichloromethane (5 × 3 mL); dichloromethane was removed under vacuum. All the products were previously reported and identification was done by comparison of their GC-MS data and ^{1}H and ^{13}C NMR spectra with the reported data.

General procedure for recycling of the catalytic phase

After extraction of the organic products, the catalytic phase was put under vacuum at 60 °C for two hours and then the appropriated reagents were added under argon to the catalytic phase. The reaction mixture was then pressurised with H_2 at the convenient pressure, heated up to the desired temperature, stirred for the appropriate time and then cooled down to room temperature. Organic products were extracted from glycerol with dichloromethane (5 × 3 mL); dichloromethane was removed under vacuum. This process is repeated for each of the different runs. All the products were previously reported and identification was done by comparison of their GC-MS data and ^{1}H and ^{13}C NMR spectra with the reported data.

Results and discussion

Synthesis and characterisation of palladium nanoparticles

We were interested in the synthesis of palladium nanoparticles (PdNPs) containing optically pure cinchona-based stabilisers in glycerol. These sustainable adsorbates coming from the biomass, exhibit the possibility to interact with both the solvent through hydrogen bonds and the metallic surface by the quinoline moiety (π-bonded and/or N-lone pair bonded).[14] Based on our previous works,[11,12] we explored the formation of PdNPs in the presence of the corresponding alkaloid (**a–d**), starting with Pd(II) and Pd(0) precursors ($Pd(OAc)_2$, **I**; $[PdCl_2(cod)]$, **II**) ($[Pd_2(dba)_3]$, **III**), under hydrogen atmosphere (3 bar) at 80 °C overnight (Scheme 1).

Cinchonidine (**a**) and quinidine (**d**) were selected as model stabilisers to choose the most appropriate metal precursor on the basis of their better catalytic activity (see below Table 1). TEM analyses of the corresponding colloidal dispersions (Table S1 in the ESI†) showed that $[Pd_2(dba)_3]$ mainly led to agglomeration and in the case of quinidine, black precipitate was formed instead of colloidal suspensions. In contrast, Pd(II) precursors gave homogeneous black solutions constituted by well-dispersed nanoparticles, in particular starting from $Pd(OAc)_2$. Therefore, PdNPs with the four alkaloids were prepared using this palladium salt. All of them yielded colloidal solutions, showing a trend to aggregate, except for **PdId** which gave a well-dispersed system (Fig. 1). However **PdIa**, **PdIb** and **PdIc** gave better dispersions after centrifugation (isolation of nanoparticles at the solid state) and re-dispersion again in glycerol (Fig. S1 in the ESI†). It is important to underline that when PdNPs at solid state were redispersed in ethanol, agglomerates and bigger nanoparticles were observed (Fig. S2 in the ESI†). These facts undeniably evidence the role of glycerol in the dispersion of nanoparticles, avoiding their aggregation, probably favoured by

Table 1 Hydrogenation of 4-phenylbut-3-en-2-one catalysed by PdNPs capped by cinchona-based stabilisers[a]

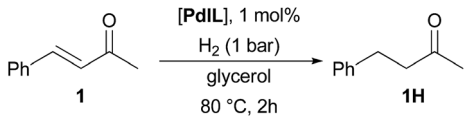

Entry	Stabiliser	Conv. (yield)[b] (%)
1	**a**	99 (96)
2	**b**	79 (74)
3	**c**	99 (90)
4	**d**	99 (98)
5	**dH**	99 (97)
6[c]	**d**	22 (21)
7[d]	**d**	99 (95)
8[e]	**TPPTS**	87 (85)

[a] Results from duplicated experiments. Reaction conditions: 1 mmol of **1** and 1 mL of the corresponding catalytic glycerol solution of PdNPs (10^{-2} mol L^{-1}, 0.01 mmol of total Pd). [b] Determined by GC and GC-MS using decane as internal standard. [c] 0.1 mol% Pd load. [d] PdNPs (1.9 mg) at solid state and redispersed in glycerol used as catalyst. [e] TPPTS = tris(3-sulfophenyl)phosphine trisodium salt.

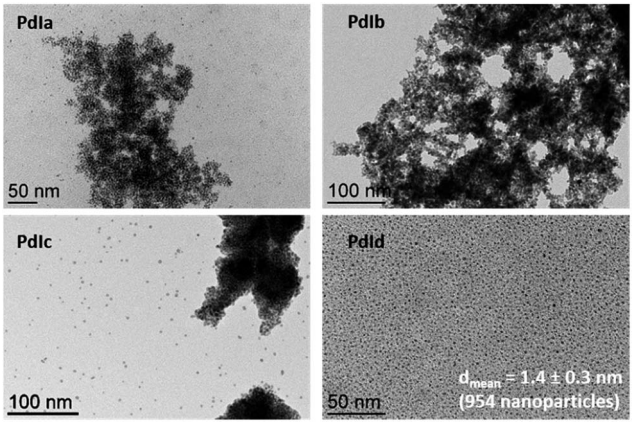

Fig. 1 TEM images in glycerol corresponding to **PdIa–PdId**.

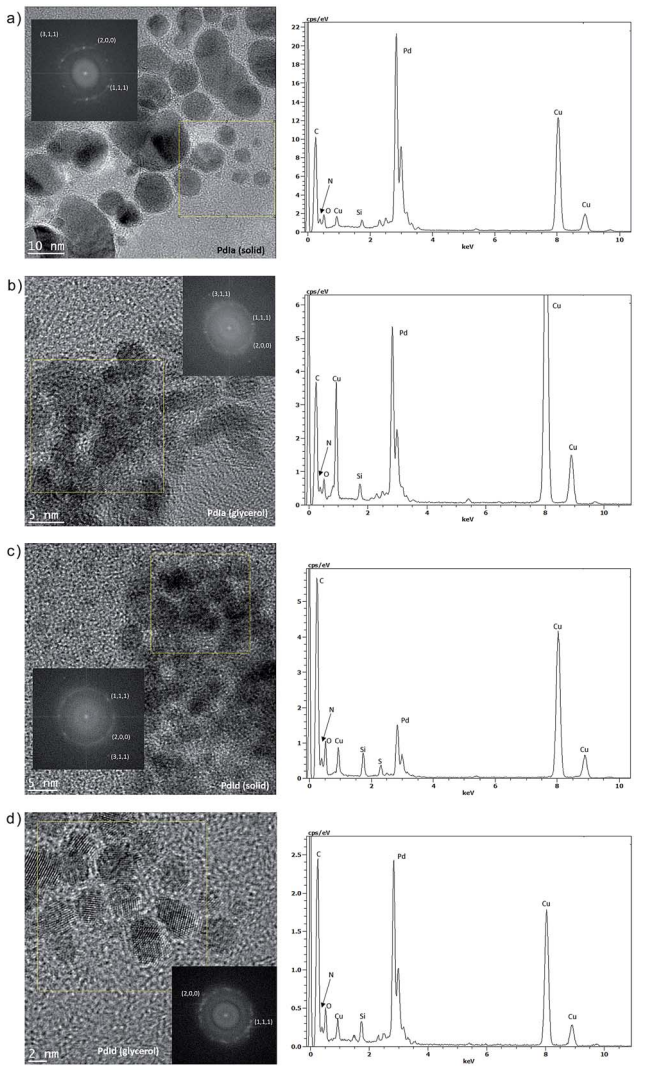

Fig. 2 HR-TEM micrographs (left) for **PdIa** (a and b) and **PdId** (c and d) at solid state (a and c) and in glycerol (b and d), with the corresponding EDX analyses (right). Crystallographic planes spots observed by Fast Fourier Transform are inserted (yellow squares represent the zone where FFT was applied).

its supramolecular arrangement due to the hydrogen bond network,[16] in agreement with our previous work using TPPTS (tris(3-sulfophenyl)phosphine trisodium salt) as stabiliser.[12a,b]

Taking into account the better dispersion of **PdId** together with the better results obtained in catalysis (see below), the formation of these PdNPs in glycerol was privileged to study the influence of different parameters on the formation of colloidal systems (hydrogen pressure, Pd/ligand ratio, temperature, metal concentration). In the absence of dihydrogen, no reduction of palladium acetate occurred, in contrast to that observed in the absence of alkaloid or in the presence of TPPTS as stabiliser, giving in both cases precipitation of black palladium.[12] Using a lower dihydrogen pressure (1 bar instead of 3 bar), only agglomerates were observed (Fig. S3 in the ESI†).

When the ligand amount in relation to metal decreased (Pd/ligand = 1/0.3 or 1/0.5), an immediate precipitation of black palladium took place. At lower temperatures (40 °C and 60 °C instead of 80 °C), colloidal solutions were attained and their TEM analyses revealed the formation of well-dispersed nanoparticles (Fig. S4 in the ESI†), but being less homogeneous in size comparing with those obtained at 80 °C (at 60 °C: $d_{mean} = 1.7 \pm 0.4$ nm; at 40 °C: $d_{mean} = 1.9 \pm 0.5$ nm). However at higher temperature (100 °C) big agglomerates were mainly formed. Concerning the metal concentration, lower concentrations (in relation to starting conditions, 10^{-2} mol L^{-1}) led to bigger nanoparticles (for [Pd] = 10^{-3} mol L^{-1}, 3.0 nm; for [Pd] = 10^{-4} mol L^{-1}, 2.4 nm); at higher concentration (0.1 mol L^{-1}), particles tended to be aggregated (Fig. S5 in the ESI†). This behaviour is in contrast to the general trend observed using common organic solvents (THF, toluene), where metal concentrations are often lower than 10^{-3} mol L^{-1},[17] what is in accordance with the supramolecular arrangement of glycerol, which favours the dispersion of nanoparticles.[16]

With the aim of checking the stability of alkaloids under synthesis conditions, we carried out a ligand exchange reaction with dodecanethiol using both **PdIa** and **PdId** in glycerol, taking advantage of the strong interaction between sulphur-based derivatives and metal surfaces (Fig. S6 in the ESI†).[18] Cinchona-based stabilisers were recovered (*ca.* 90% yield) by biphasic extraction as a mixture of the corresponding alkaloid and its dihydro-cinchona partner, it means hydrocinchonidine (**aH**) and hydroquinidine (**dH**), due to the anticipated hydrogenation of the vinyl group under dihydrogen atmosphere (**a**/**aH** = 1.3/1; **d**/**dH** = 2/1, Fig. S6 in the ESI†).[19] No modification of the quinoline fragment was observed, preserving the adsorption of the ligand at the metallic surface through π- or N-lone pair bound interactions and in consequence avoiding agglomeration during the PdNPs synthesis.[14]

It is expected that this structural change on the cinchona ligands triggers minor effect on the stabilisation of PdNPs and in the subsequent catalytic activity. Actually, PdNPs capped by hydroquinidine (named **PdIdH**) exhibited spherical dispersed nanoparticles (mean diameter: 2.5 ± 0.9 nm), but tending to be more agglomerated than those prepared from quinidine (Fig. S8 in the ESI†). Moreover, no differences were observed in hydrogenation and hydrodebromination reactions in comparison with the system **PdId** (see Catalytic applications section and Scheme S1 in the ESI†).

The composition of **PdIa** and **PdId** at solid state was determined by ICP (Pd) and elemental analysis (C, H, N) (see Experimental section), indicating a Pd/alkaloid ratio of 2.2 and 2.4 for **PdIa** and **PdId**, respectively. With the purpose of estimating the content of hydrides, **PdIa** and **PdId** at solid state were dispersed in THF-d_8, in the presence of one equivalent of maleic anhydride; the corresponding mixtures were monitored by ^{1}H NMR (cyclooctane used as internal standard), without observing any evolution after the first hour.[20] For both materials, a Pd/H ratio of *ca.* 2/1 was found (Fig. S9 in the ESI†). With this analytical data and the mean diameter found by TEM analysis (Fig. 1 and S1 in the ESI†), nanoclusters of idealized formula $Pd_{309}L_{129}H_{155}$ and $Pd_{147}L_{61}H_{74}$ can be proposed for **PdIa** and **PdId**, respectively (L means the corresponding cinchona stabiliser).[21]

IR spectra showed the presence of the alkaloid in the isolated **PdIa** and **PdId** (Fig. S10 in the ESI†). No important differences were observed between the free cinchona-based ligand and the corresponding PdNPs, pointing probably to an N-lone pair interaction between the stabiliser and the metallic surface more than a π-binding coordination.[14]

Powder XRD analyses of **PdIa** and **PdId** exhibited the peaks corresponding to the fcc Pd(0) structure, without observing crystalline Pd(II) phases (Fig. S11 in the ESI†). HR-TEM at solid state also evidenced this structure (Fig. 2). The surface composition and the electronic state of the PdNPs were studied by XPS spectroscopy. XPS survey spectra for both solid materials **PdIa** and **PdId** showed the presence of palladium, carbon, oxygen and nitrogen (Fig. S12 in the ESI†). The high-resolution spectra in the binding energy region corresponding to palladium (Pd $3d_{3/2}$ and Pd $3d_{5/2}$) showed the merely presence of Pd(0), in agreement with the data obtained by XRD (Fig. S13 in the ESI†).[22] For the N 1s binding region, only one signal was observed, consistent with the XPS analyses of neat ligands (*i.e.* the electronic differences between both nitrogen atoms, *N*-quinuclidine and *N*-quinoline, could not be distinguished by XPS in agreement with the reported data[23]) (Fig. S14 in the ESI†).

With the aim of elucidating the structure of PdNPs in solution, **PdIa** and **PdId** dispersed in glycerol (colloidal solutions) were also directly analysed by HR-TEM, EDX and XPS taking advantage of the negligible vapour pressure of glycerol. HR-TEM and EDX analyses proved both the fcc Pd structure for the nanoclusters dispersed in glycerol and the presence of the stabiliser (Fig. 2).

XPS analyses of the colloidal solutions evidenced the absence of Pd(II) species (for the survey XPS spectra, see Fig. S15 in the ESI†); actually, HR-XPS spectra only showed the corresponding binding energies for Pd(0) (Fig. 3). In contrast to the PdNPs isolated at solid state (see above), two binding energies were observed in the region of N 1s, probably due to both types of alkaloid molecules present in the colloidal solution, those linked to the surface and those solvated by glycerol. Actually, we analysed by ^{15}N NMR neat quinidine both in the absence and in the presence of glycerol. As expected, two signals were observed corresponding to the nitrogen atoms from quinoline and quinuclidine moieties in deuterated methanol. However in a mixture of CD_3OD/glycerol (1/1) only the ^{15}N chemical shift corresponding to quinoline was observed, probably due to the enlargement of the signal corresponding to the quinuclidine nitrogen by hydrogen bond interaction with glycerol (Fig. S16 in the ESI†).[13g] This behaviour could explain the two types of molecules consistent with the signals observed by XPS in the N 1s region.

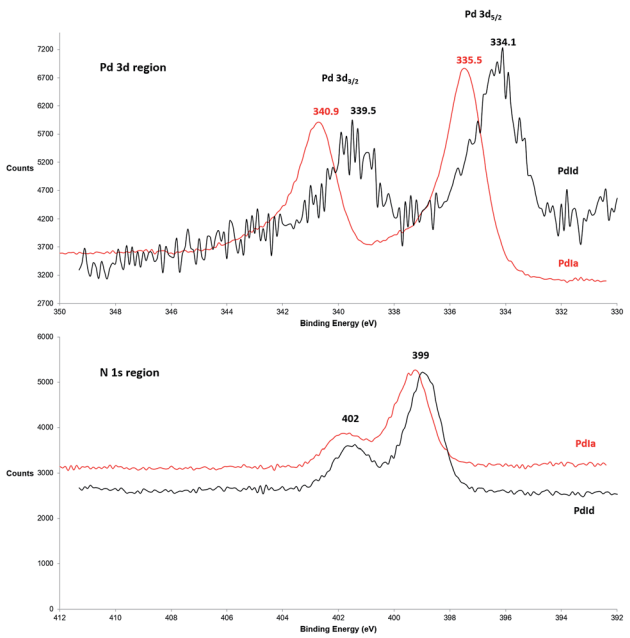

Fig. 3 High-resolution XPS spectra for **PdIa** and **PdId** in glycerol: (a) Pd 3d binding energy region; (b) N 1s binding energy region.

Catalytic applications

Due to the surface reactivity of PdNPs,[6,24] we were interested in the evaluation of their behaviour in dihydrogen-based processes, such as hydrogenation of unsaturated functional groups (alkenes, alkynes, imines, nitro-based substrates) and hydrodehalogenation reactions, because of their industrial applications.

Hydrogenation reactions. We chose the hydrogenation of 4-phenylbut-3-en-2-one (**1**) as benchmark reaction to compare the reactivity of the different PdNPs stabilised by the corresponding alkaloids in glycerol (entries 1–5, Table 1). For all of them, only 4-phenylbutan-2-one (**1H**) was exclusively obtained. No important differences in reactivity among the PdNPs catalysts were found, except for cinchonine (**b**, entry 2), which gave lower conversion. The partially hydrogenated quinidine **dH** (see above) led to the same reactivity trend than its vinyl-based partner **d** (entry 5 *vs.* 4), indicating that the structural modification on the stabiliser **d** does not trigger a different catalytic behaviour of the corresponding PdNPs. **PdId** was active even at very low load of catalyst (0.1 mol%) under the same conditions (1 bar H_2, 80 °C, 2 h; entry 6). **PdId** at solid state was also used as catalytic precursor, finding the same catalytic activity than for the colloidal system (entry 7 *vs.* 1). PdNPs stabilised by the phosphine TPPTS[12a,b] gave slightly lower conversion and yield than for the cinchona capped nanoparticles (entry 8 *vs.* entries 1, 3–5 and 7).

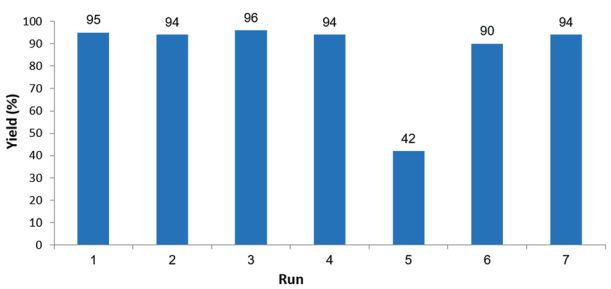

Fig. 4 Diagram showing the recycling of the catalytic phase **PdId** for the hydrogenation of 4-phenylbut-3-en-2-one (Table 1). Figures indicate yields of **1H** (determined by GC).

Table 2 Hydrogenation of compounds containing C=C or C≡C bonds catalysed by **PdId**[a]

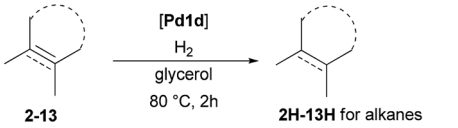

Entry	Substrate	Product	Pd mol% (pH_2)	Conv. (yield)[b] (%)
1	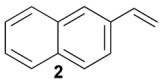 **2**	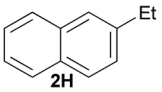 **2H**	0.1[c] (1)	>99 (99)
2	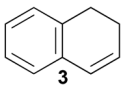 **3**	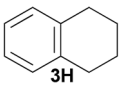 **3H**	0.1[c] (1)	94 (90)
3	 **4**	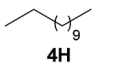 **4H** 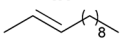 **4I**	1 (1)	90 (3/1)[d]
4	 **4**	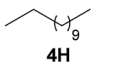 **4H** 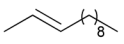 **4I**	1 (3)	99 (94)[e] (99/1)
5	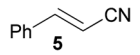 **5**	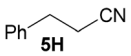 **5H**	1 (1)	97 (94)
6	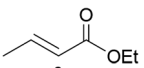 **6**	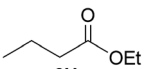 **6H**	1 (1)	>99 (96)
7	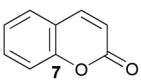 **7**	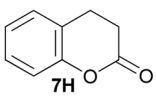 **7H**	1 (10)	85 (79)
8	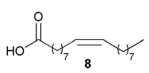 **8**	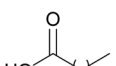 **8H**	1 (1)	>99 (94)
9	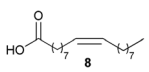 **8**	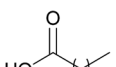 **8H**	0.1[c] (1)	48 (46)[f]
10	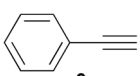 **9**	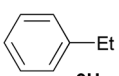 **9H**	0.5[g] (1)	>99 (95)
11	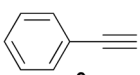 **9**	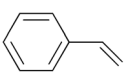 **9HE**	0.1[c] (1)	98 (90)[h]
12	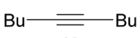 **10**	 **10H**	1 (3)	>99 (90)[i]
13	 **10**	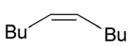 **10HE**	0.5[g] (1)	>99 (96)[i]
14	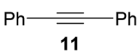 **11**	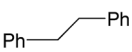 **11H**	0.5[g] (1)	>99 (96)
15	 **11**	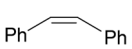 **11HE**	0.1[c] (1)	47 (41)
16	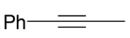 **12**	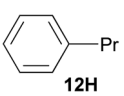 **12H**	1 (3)	>99 (97)

Table 2 (*Contd.*)

Entry	Substrate	Product	Pd mol% (pH_2)	Conv. (yield)[b] (%)
17	Ph— ≡ **12**	**12HE**	0.5[g] (1)	45 (40)[j]

[a] Results from duplicated experiments. Reaction conditions: 1 mmol of substrate (**2–12**) and 1 mL of the catalytic glycerol solution of **PdId** (10^{-2} mol L^{-1}, 0.01 mmol of total Pd). See Table S2 in the ESI for the results using **PdIa** as catalyst. [b] Determined by GC and GC-MS using decane as internal standard. [c] 10 mmol of substrate for 1 mL of the catalytic solution (0.01 mmol of total Pd). [d] In brackets, **4H**/**4I** ratio. [e] For 12 h. [f] At 30 °C for 24 h. [g] 5 mmol of substrate for 1 mL of the catalytic solution (0.01 mmol of total Pd). [h] 5% of **9H** was detected. [i] Cyclooctane used as internal standard. [j] At 35 °C for 6 h.

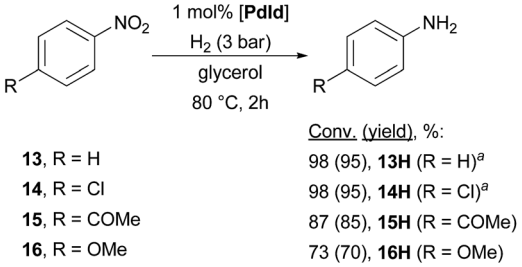

13, R = H — Conv. (yield), %: 98 (95), **13H** (R = H)[a]
14, R = Cl — 98 (95), **14H** (R = Cl)[a]
15, R = COMe — 87 (85), **15H** (R = COMe)
16, R = OMe — 73 (70), **16H** (R = OMe)

Scheme 2 Pd-catalysed hydrogenation of nitro-arenes by PdId nanoparticles in glycerol ([Pd] = 10^{-2} mol L^{-1}). Conversions and yields were determined by GC and GC-MS, using decane as internal standard ([a] denotes the use of 0.5 mol% **PdId**).

The catalytic glycerol phase **PdId** was recycled four times showing the same catalytic behaviour. After the activity decrease on the 5th run, the catalytic solution was treated under H_2 (3 bar) overnight and then reused, recovering its activity (Fig. 4). Palladium was no detected in the isolated 4-phenylbutan-2-one after the different runs (the palladium load was lower than the detection limit by ICP-AES, *i.e.* <0.01 ppm). TEM analyses after the first and fourth runs did not evidence any sign of agglomeration, remaining the nanoparticles well dispersed but showing a bigger size in relation to the starting catalytic solution (*ca.* 2.0 nm – Fig. S17 in the ESI† – *vs.* 1.4 nm – Fig. 1).

Using **PdId** as catalyst (with **PdIa**, a similar catalytic behaviour could be observed; see Table S2 in the ESI†), compounds containing C=C or C≡C bond were efficiently reduced (Table 2). Therefore, non-functionalised alkenes, both conjugated (**2**, **3**) and non-conjugated (**4**) C=C bonds, were hydrogenated. Substrates **2** and **3** reacted using only 0.1 mol% of catalyst (entries 1–2). In the case of 1-dodecene (**4**), the isomerisation towards the internal alkene 2-dodecene could be also observed (entry 3); working at higher pressure (3 bar) and longer time (12 h) dodecane was merely isolated (entry 4). Polyfunctionalised C=C based substrates such as cinnamonitrile (**5**) and ethylcrotonate (**6**) led to the hydrogenation of the corresponding C=C bond (entries 5 and 6, respectively). However for the endocyclic C=C bond hydrogenation of coumarin (**7**), higher pressure (10 bar H_2) was required to get *ca.* 80% yield of the corresponding hydrogenated product, **7H** (entry 7).

We also evaluated the hydrogenation of oleic acid (entry 8), because of the industrial interest of saturated fatty acids (*e.g.* as surfactants (soaps, detergents, cosmetics) or lubricants). Remarkably, no esterification products with glycerol were detected and the extraction of the corresponding hydrogenated compound (stearic acid) from the glycerol catalytic phase (by means of a biphasic extraction, adding dichloromethane) easily worked (entry 8). The reaction also ran under very smooth conditions (0.1 mol% **PdId**, 30 °C, 24 h, 1 bar H_2; entry 9). These catalysts were also applied in the hydrogenation of terminal (**9**) and internal (**10–12**) alkynes. Tuning the catalytic conditions, we could selectively achieve the reduction towards the corresponding alkene or alkane. Actually, at low palladium load (0.1–0.5 mol% depending on the alkyne) and low dihydrogen pressure (1 bar) the corresponding alkene was chemoselectively formed (entries 11, 13, 15 and 17). At relative harsher conditions (0.5–1.0 mol% Pd and 1–3 bar H_2), the fully hydrogenated products were only obtained (entries 10, 12, 14 and 16). The NOESY-NMR analysis of **12HE** revealed the exclusive formation of the (*Z*)-stereoisomer (Fig. S18 in the ESI†), indicating a dihydrogen *syn* addition on the C≡C bond, as expected for a Pd surface-like mechanism. Unluckily, no asymmetric induction could be observed for the hydrogenation of prochiral substrates, such as ethyl pyruvate, dimethyl itaconate or isophorone (Fig. S19 in the ESI†).

Anilines could be easily obtained by hydrogenation of the corresponding nitro-arene starting materials, **13–16** (Scheme 2).

The reaction seems to be more sensitive to steric than electronic effects on the substrate. In fact, nitrobenzene (**13**) and 4-chloronitrobenzene (**14**) were more active than 4-nitroacetophenone (**15**) and 4-nitroanisole (**16**), getting 95% of the corresponding aniline, **13H** and **14H**, using only 0.5 mol% **PdId**. Working under higher hydrogen pressure (10 bar H_2) and temperature (100 °C) some extent of hydrodechlorination was detected (*ca.* 10% of formation of nitrobenzene) for 4-chloronitrobenzene (see below).

This scope proves that PdNPs stabilised by cinchona-based alkaloids cannot reduce ketone, ester or carboxylic acid functions. For the tested aromatic ketones (**17–19**), only acetophenone gave the corresponding secondary alcohol, 1-phenylethanol, leading to less than 30% conversion working under harsher conditions (80 °C under 20 bar H_2 for 24 h) (Scheme S2 in the ESI†); no formation of the corresponding acetal derivative by reaction of the carbonyl group with glycerol was detected. We also studied the ability of these catalysts on the hydrogenation of

Table 3 Pd-catalysed synthesis of secondary and tertiary amines from carbonyl and amine reagents under hydrogen pressure[a]

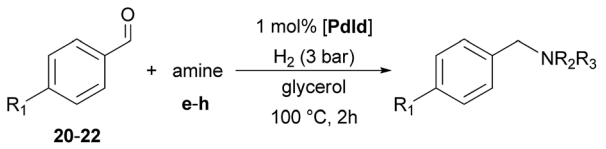

20-22

Entry	R_1	Amine	Product	Conv. (yield)[b] (%)
1	OMe (**22**)	Cy-NH_2 (**e**)	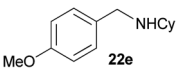 **22e**	93 (91)
2	OMe (**22**)	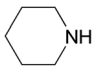 **f**	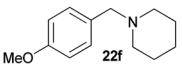 **22f**	81 (77)
3	OMe (**22**)	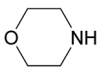 **g**	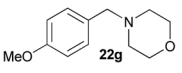 **22g**	77 (73)
4	H (**20**)	Cy-NH_2 (**e**)	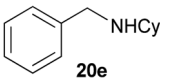 **20e**	99 (96)
5	CF_3 (**21**)	Cy-NH_2 (**e**)	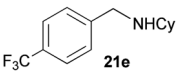 **21e**	98 (95)
6	H (**20**)	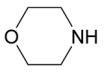 **g**	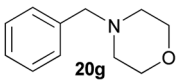 **20g**	78 (76)
7	CF_3 (**21**)	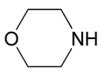 **g**	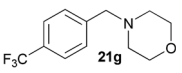 **21g**	80 (76)
8	H (**20**)	NH_3[c] (**h**)	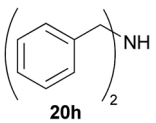 **20h**	62 (40)[d]
9	OMe (**22**)	NH_3[c] (**h**)	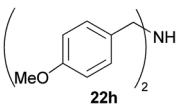 **22h**	91 (56)[e]
10[f]	CF_3 (**21**)	NH_3[c] (**h**)	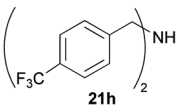 **21h**	95 (91)

[a] Results from duplicated experiments. Reaction conditions: 1 mmol of aldehyde (**20–22**), 1 mmol of the corresponding amine (**e–h**) and 1 mL of the catalytic glycerol solution of **PdId** (10^{-2} mol L^{-1}, 0.01 mmol of total Pd), under 3 bar of H_2 at 100 °C for 2 h. [b] Determined by GC and GC-MS using decane as internal standard. [c] 32% w/w aqueous solution NH_3 (55 μL, 1 mmol). [d] 20% of tris(benzyl)amine was also obtained. [e] 34% of the corresponding tris(benzyl)amine was also obtained, N(4-OMe-C_6H_4)$_3$. [f] For 12 h.

aldehydes (**20–23**). Only benzaldehyde was hydrogenated to give benzyl alcohol (60% yield) but in this case under relative smooth conditions (Scheme S2 in the ESI†). In contrast to acetophenone, the five-membered acetal coming from benzaldehyde and glycerol was obtained as by-product in *ca.* 30% yield.

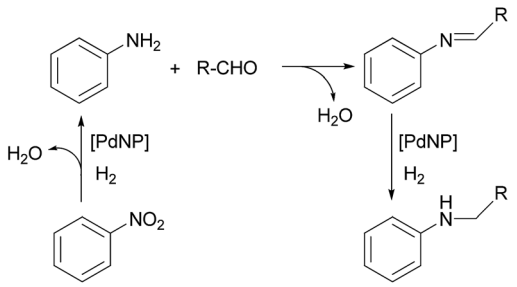

Scheme 3 One-pot multi-step synthesis of *N*-substituted anilines catalysed by PdNPs in glycerol.

In order to get a deeper insight in the synthesis of primary and secondary amines from nitro-compounds, we envisaged the one-pot procedure by reaction of amine and carbonyl-based reactants in the presence of PdNPs under hydrogen atmosphere, taking advantage of the lack or low reactivity of ketones and aldehydes compounds (Table 3). This procedure obviously involves the *in situ* formation of an imine (condensation between primary amine and aldehyde or ketone) or iminium (condensation involving a secondary amine) intermediate.[25] We previously proved the efficiency of **PdIa** and **PdId** on the reduction of imines using *N*-benzylideneaniline (**24**) as model imine-based substrate (Scheme S3 in the ESI†). We chose 4-methoxybenzaldehyde (**22**) as model substrate (entries 1–3, Table 3), which was not hydrogenated with the catalysts used (see above), using primary (cyclohexylamine, **e**) and secondary (piperidine and morpholine, **f** and **g** respectively) amines. Conversions and yields were high, but somewhat lower for secondary amines than for cyclohexylamine (entries 2–3 *vs.* 1). The same trend was observed for benzaldehyde and 4-(trifluoromethyl)benzaldehyde (entries 4–5 and 6–7), proving that electronic effects are no significant. In the case of cyclohexylamine, the corresponding tertiary amines were not formed, even using an excess of aldehyde (entries 1, 4 and 5); this behaviour points to the fact that the secondary amines **20e–22e** are sterically demanding enough to avoid the formation of the corresponding iminium intermediate (entries 1, 4 and 5), in contrast to that observed for piperidine and morpholine (entries 2–3 and 6–7). We also evaluated the reactivity involving ammonia (**h**) instead of organic amines (entries 8–10). In this case, we observed an influence of the aldehyde nature. Using benzaldehyde (**20**) and 4-methoxybenzaldehyde (**22**), a mixture of the corresponding secondary and tertiary amines were obtained (entries 8 and 9), while with 4-(trifluoromethyl)benzaldehyde (**21**), the secondary amine **21h** was exclusively formed in high yield (91%, entry 10). This behaviour proves that aldehydes containing electron-withdrawing groups favour the formation of the corresponding imine, but the iminium intermediate is disfavoured as can be expected (Scheme S4 in the ESI†). Unfortunately ketones were not reactive.

Following this line-up, we could prepare *N*-substituted anilines by one-pot three-steps sequential process;[26] it means the reduction of nitrobenzene, then the formation of the corresponding imine by condensation with the appropriate

Table 4 Pd-catalysed one-pot synthesis of *N*-substituted anilines from nitrobenzene and aldehydes under hydrogen pressure[a]

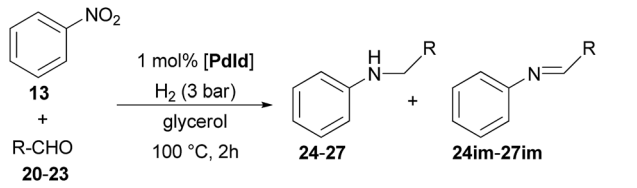

Entry	R	Conv.[b] (%)	Products *N*-aniline/imine[b] (yields, %)
1	Ph (**20**)	>99[c]	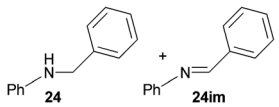 87 / 5
2	4-CF_3-C_6H_4 (**21**)	97	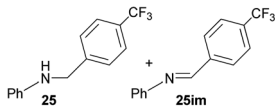 75 / 20
3	4-OMe-C_6H_4 (**22**)	>99	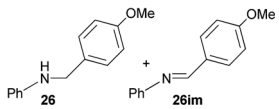 90 / 5
4	Bu (**23**)	86[d]	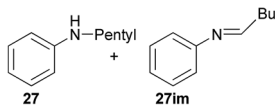 72 / 10

[a] Results from duplicated experiments. Reaction conditions: 1 mmol of aldehyde (**20–23**), 1 mmol of nitrobenzene and 1 mL of the catalytic glycerol solution of **PdId** (10^{-2} mol L^{-1}, 0.01 mmol of total Pd), under 3 bar of H_2 at 100 °C for 2 h. [b] Determined by GC and GC-MS using decane as internal standard. [c] 20% of Bn–OH. [d] *ca.* 5% of *N*,*N*-bis(pentyl)-*N*-phenyl-amine.

aldehyde, followed by its hydrogenation to give the *N*-substituted aniline (Scheme 3).

We applied this strategy using aromatic- (**20–22**) and alkyl- (**23**) aldehydes (Table 4). We mainly observed in all the cases the formation of the anticipated secondary amine (**24–27**, entries 1–4). The corresponding imine (**24im–27im**) could be also detected, in particular for 4-(trifluoromethyl)benzaldehyde, up to 20% (entry 2). In the case of pentanal, two by-products were detected together with *N*-pentyl-*N*-phenylamine **27** (72%); in addition to the imine **27im** (10%), the tertiary amine *N*,*N*-bis(-pentyl)-*N*-phenyl-amine was also formed (5%, entry 4), in contrast to the behaviour observed for the secondary benzyl-amines **24–26**.

Hydrodehalogenation processes. We were also interested in Pd-catalysed hydrodehalogenation of haloarenes, important concern in the treatment of wastes. Halogen compounds are typically xenobiotic which presume a negative environmental impact. Catalytic hydrodehalogenation mediated by dihydrogen represents a sustainable approach as alternative of incineration, involving cleavages of C–X bonds which can lead to less toxic and recyclable materials.[27]

Table 5 Pd-catalysed hydrodebromination processes under hydrogen pressure[a]

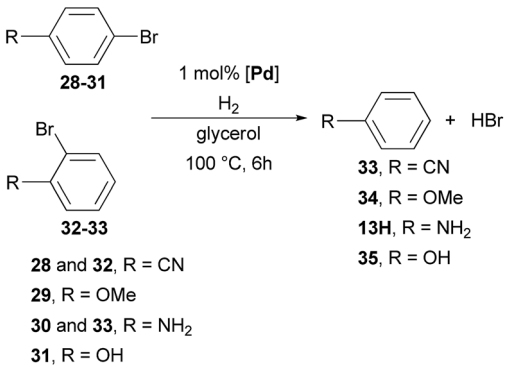

Entry	Catalyst	Substrate	pH_2 (bar)	Conv. (yield)[b] (%)
1	**PdIa**	**28**	3	25 (15)
2	**PdId**	**28**	3	99 (94)
				99 (94) 2nd run
				97 (93) 3rd run
				92 (89) 4th run
3	**PdIdH**	**28**	3	99 (91)
4[c]	**PdTPPTS**	**28**	3	<5
5[d]	**PdId**	**28**	3	40 (36)
6	**PdId**	**29**	3	<5
7	**PdId**	**30**	3	<5
8	**PdId**	**31**	3	<5
9[e]	**PdId**	**29**	10	67 (65)
10[e]	**PdId**	**30**	10	89 (86)
11[e]	**PdId**	**31**	10	68 (65)
12	**PdId**	**32**	3	38 (32)
13	**PdId**	**33**	3	<5
14	**PdId**	**32**	10	77 (71)
15	**PdId**	**33**	10	10 (nd)[f]
16[g]	**PdId**	**31**	3	98 (95)
17[h]	**Pd/C**	**31**	3	97 (94)
				45 (40) 2nd run
18[g,h]	**Pd/C**	**31**	3	98 (94)

[a] Results from duplicated experiments. Reaction conditions: 1 mmol of aryl-halide (**28–33**) and 1 mL of the corresponding catalytic glycerol solution (10^{-2} mol L^{-1}, 0.01 mmol of total Pd), under 3 or 10 bar of H_2 at 100 °C for 6 h. [b] Determined by GC and GC-MS using decane as internal standard. [c] TPPTS = tris(3-sulfophenyl)phosphine trisodium salt. [d] At 80 °C. [e] For 24 h. [f] nd = not determined. [g] For 2 h in the presence of 1.2 mmol of KOH. [h] Pd/C 10 wt 10% (Aldrich).

We selected 4-bromobenzonitrile for evaluating the ability of our catalysts in the hydrodehalogenation process (Table 5). Under 3 bar H_2 pressure at 100 °C for 6 h using 1 mol% of catalyst (entries 1–4), we could observe that the best results were achieved with **PdId** and **PdIdH**: full conversion with more than 90% yield in benzonitrile (entries 2–3), in contrast to the low reactivity observed using **PdIa** as catalyst (entry 1). **PdId** could be recycled four times without loss of reactivity (entry 2). PdNPs stabilised by TPPTS were inactive (entry 4).[12a,b] Lower

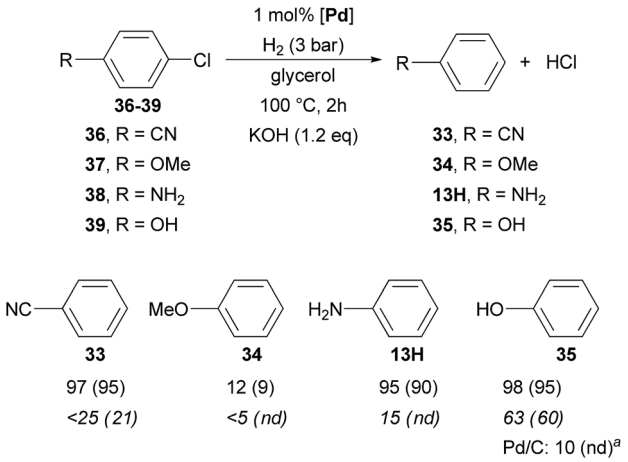

Scheme 4 Hydrodechlorination catalysed by PdNPs in glycerol. Figures represent conversions and yields (in brackets) using **PdId** as catalyst; in italics, data corresponding using **PdIa** (nd = not determined). [a]In the absence of KOH, 48% conversion (45% yield).

temperatures affected markedly the conversion (entry 5 *vs.* 2). Under smooth conditions, 4-bromoanisole (**29**), 4-bromoaniline (**30**) and 4-bromophenol (**31**) did not react (entries 6–8), obtaining the corresponding debrominated compound under harsher conditions (10 bar of H_2 for 24 h), in moderate to good yields (65–86% yields, entries 9–11). Using 2-bromobenzonitrile and 2-bromoaniline as substrates, the activity was negligible, as consequence of the steric hindrance (entries 12–13). The pressure increase (10 bar H_2) gave 77% conversion towards benzonitrile (entry 14), but only 10% of conversion was observed for the hydrodebromation of 2-bromoaniline (entry 15), indicating that electro-donor groups slowed down the process, as observed for **29–31** in comparison with 4-bromobenzonitrile (entries 9–11 *vs.* 2).

With the aim of improving the hydrodehalogenation under relative low H_2 pressure, we then decided to add a base in the medium in order to trap the hydrogen bromide formed as concomitant product.[28] Under these basic conditions, 95% yield of phenol was obtained from 4-bromophenol working under 3 bar H_2 at 100 °C for 2 h (entry 16 *vs.* 8). For comparative purposes, the dehydrodebromination of 4-bromophenol (**31**) was conducted using the heterogeneous Pd/C catalyst both in the absence and in the presence of base (entries 17 and 18, respectively), leading to the same reactivity (95% yield of phenol), likewise to **PdId** (entry 16). But the activity fell after reuse of the heterogeneous catalyst (entry 17), in contrast to the colloidal catalyst (entry 2). It is important to mention that the stabiliser (quinidine, **d**) remains unmodified after catalysis, as checked by ^{1}H NMR (for catalytic conditions, see entry 2 of Table 5).[29]

More challenging substrates are chloro-arenes. At 100 °C under 10 bar H_2 for 24 h, 4-chlorobenzonitrile (**36**), 4-chloroanisole (**37**), 4-chloroaniline (**38**) and 4-chlorophenol (**39**) were inactive using both **PdIa** and **PdId** (1 mol%) as catalysts, in the absence of base. However in the presence of KOH and working under smoother conditions (100 °C, 3 bar H_2, 2 h), yields up to 95% were achieved with **PdId** except for **37** which gave only 12% conversion (Scheme 4); **PdIa** was much less active (Scheme 4). In contrast to the behaviour observed for hydrodebromination, Pd/C was less efficient than **PdId** giving up to 48% of phenol in the absence of base; in the presence of KOH, only 10% conversion was achieved (for conditions, see Scheme 4). These results points to a poisoning of the heterogeneous catalyst by the base in glycerol, oppositely to the beneficial effect triggered on the nanocatalyst **PdId**.

Conclusions

In summary, we prepared palladium nanoparticles capped by cinchona-based ligands in neat glycerol. Important effects in size and dispersion of PdNPs were observed, depending on the palladium precursor involved and also the nature of stabiliser. The most homogeneously dispersed systems showing a small size (*ca.* 1.5–2.0 nm) were those stabilised by cinchonidine (**a**) and quinidine (**d**), using palladium acetate as metal precursor, **PdIa** and **PdId** respectively. The characterisation, both at solid state and in the glycerol phase, evidenced that only Pd(0) was present in any case. Cinchona-based ligands are linked at the metal surface in solution and in solid state, probably adopting a relative weak interaction with the metal surface through N-lone pair of the quinolone ring more than a π-binding coordination, in agreement with the literature.[14] In glycerol phase, both solvated quinidine and quinidine linked to the metal surface were identified by XPS and ^{15}N NMR analyses. **PdIa** and **PdId** dispersed in glycerol were successfully applied in dihydrogen-based processes, such as hydrogenation of unsaturated functional groups (alkenes, alkynes, imines, nitro-based substrates) and hydrodehalogenation of halo-aromatic compounds, taking advantage of their surface-like reactivity. Glycerol played an important role as support for the immobilisation of PdNPs, permitting an easy recycling of the catalytic phase. The versatile behaviour of these catalysts, mainly **PdId**, allowed the synthesis of secondary and tertiary amines, and *N*-substituted anilines by a one-pot methodology without isolation of intermediates.

Further studies involving metal-based nanoparticles in glycerol containing naturally-occurring stabilisers are currently developed for applications in organic synthesis.

Acknowledgements

Financial support from the Centre National de la Recherche Scientifique (CNRS), the Université de Toulouse 3 – Paul Sabatier, the Associated International Laboratory LIA-LCMMC and CONACYT FOINS-246968 are gratefully acknowledged. Authors thank L. Calvo for his helpful discussions concerning XPS data. A. R. thanks CONACYT for a PhD grant.

Notes and references

1 For a selected contribution, see: J. Tsuji, *Palladium reagents and catalysts*, John Wiley & Sons, Sussex, 2004.

2 For selected reviews, see: (*a*) R. Ciriminna, V. Pandarus, A. Fidalgo, L. M. Ilharco, F. Béland and M. Pagliaro, *Org. Process Res. Dev.*, 2015, **19**, 755; (*b*) S. Paul, M. M. Islam and S. M. Islam, *RSC Adv.*, 2015, **5**, 42193; M. Opanasenko, P. Stepnicka and J. Cejka, *RSC Adv.*, 2014, **4**, 65317. (*c*) P. Taladriz-Blanco, P. Herves and J. Pérez-Juste, *Top. Catal.*, 2013, **56**, 1154; (*d*) M. O. Sydnes, *Curr. Org. Synth.*, 2011, **8**, 881; (*e*) I. Beletskaya and V. Tyurin, *Molecules*, 2010, **15**, 4792.

3 For selected contributions, see: (*a*) D. J. Gavia and Y.-S. Shon, *ChemCatChem*, 2015, **7**, 892; (*b*) F. Chahdoura, I. Favier and M. Gómez, *Chem.–Eur. J.*, 2014, **20**, 10884; (*c*) S. Navalon, M. Alvaro and H. Garcia, *ChemCatChem*, 2013, **5**, 3460; (*d*) J. D. Scholten, B. C. Leal and J. Dupont, *ACS Catal.*, 2012, **2**, 184; (*e*) M. H. G. Prechtl, J. D. Scholten and J. Dupont, in *Palladium Nanoscale Catalysts in Ionic Liquids: Coupling and Hydrogenation Reactions (Chapter 16) from Ionic Liquids: Applications and Perspectives*, ed. A. Kokorin, InTech, 2011, pp. 393–414.

4 For selected contributions, see: (*a*) R. Rossi, F. Bellina, M. Lessi, C. Manzini, G. Marianetti and L. A. Giulia, *Curr. Org. Chem.*, 2015, **19**, 130; (*b*) B. M. Trost, *Tetrahedron*, 2015, **71**, 5708; (*c*) Y. Liu, S.-J. Han, W.-B. Liu and B. M. Stoltz, *Acc. Chem. Res.*, 2015, **48**, 740; (*d*) D.-L. Mo, T.-K. Zhang, G.-C. Ge, X.-J. Huang, C.-H. Ding, L.-X. Dai and X.-L. Hou, *Synlett*, 2014, **25**, 2686; (*e*) C. Deraedt and D. Astruc, *Acc. Chem. Res.*, 2014, **47**, 494; (*f*) A. Balanta, C. Godard and C. Claver, *Chem. Soc. Rev.*, 2011, **40**, 4973; (*g*) I. Favier, D. Madec, E. Teuma and M. Gómez, *Curr. Org. Chem.*, 2011, **15**, 3127.

5 For selected contributions, see: (*a*) A. Bej, K. Ghosh, A. Sarkar and D. W. Knight, *RSC Adv.*, 2016, **6**, 11446; (*b*) I. Saldan, Y. Semenyuk, I. Marchuk and O. Reshetnyak, *J. Mater. Sci.*, 2015, **50**, 2337; (*c*) V. P. Ananikov and I. P. Beletskaya, *Organometallics*, 2012, **31**, 1595; (*d*) M. Pérez-Lorenzo, *J. Phys. Chem. Lett.*, 2012, **3**, 167; (*e*) A. Fihri, M. Bouhrara, B. Nekoueishahraki, J.-M. Basset and V. Polshettiwar, *Chem. Soc. Rev.*, 2011, **40**, 5181; (*f*) D. Astruc, *Inorg. Chem.*, 2007, **46**, 1884.

6 (*a*) N. T. S. Phan, M. V. Sluys and C. W. Jones, *Adv. Synth. Catal.*, 2006, **348**, 609; (*b*) J. Durand, E. Teuma and M. Gómez, *Eur. J. Inorg. Chem.*, 2008, 3577; D. Astruc, F. Lu and J. R. Aranzaes, *Angew. Chem., Int. Ed.*, 2005, **44**, 7852.

7 (*a*) C. S. Consorti, P. A. Z. Suarez, R. F. de Souza, R. A. Burrow, D. H. Farrar, A. J. Lough, W. Loh, L. H. M. da Silva and J. Dupont, *J. Phys. Chem. B*, 2005, **109**, 4341; (*b*) J. Dupont, *J. Braz. Chem. Soc.*, 2004, **15**, 341; (*c*) I. Favier, D. Madec and M. Gómez, in *Metallic nanoparticles in ionic liquids – Applications in catalysis (Chapter 5) from Nanomaterials in Catalysis*, ed. P. Serp and K. Philippot, Wiley-VCH, Weinheim, 2013, pp. 203–249.

8 (*a*) A. J. Biacchi and R. E. Schaak, *ACS Nano*, 2011, **5**, 8089; (*b*) I. Favier, E. Teuma and M. Gómez, *C. R. Chim.*, 2009, **12**, 533.

9 For a selected review, see: I. Geukens and D. E. De Vos, *Langmuir*, 2013, **29**, 3170.

10 For selected reviews, see: (*a*) C. Amiens, D. Ciuculescu-Pradines and K. Philippot, *Coord. Chem. Rev.*, 2016, **308**, 409; (*b*) E. Gross and G. A. Somorjai, *J. Catal.*, 2015, **328**, 91; (*c*) A. Roucoux, J. Schulz and H. Patin, *Chem. Rev.*, 2002, **102**, 3757.

11 F. Chahdoura, C. Pradel and M. Gómez, *ChemCatChem*, 2014, **6**, 2929.

12 (*a*) F. Chahdoura, C. Pradel and M. Gómez, *Adv. Synth. Catal.*, 2013, **355**, 3648; (*b*) F. Chahdoura, S. Mallet-Ladeira and M. Gómez, *Org. Chem. Front.*, 2015, **2**, 312; (*c*) F. Chahdoura, I. Favier, C. Pradel, S. Mallet-Ladeira and M. Gómez, *Catal. Commun.*, 2015, **63**, 47.

13 (*a*) P. J. Collier, J. A. Iggo and R. Whyman, *J. Mol. Catal. A: Chem.*, 1999, **146**, 149; (*b*) M. F. Dumont, S. Moisan, C. Aymonier, J.-D. Marty and C. Mingotaud, *Macromoleucles*, 2009, **42**, 4937; (*c*) E. Schmidt, W. Kleist, F. Krumeich, T. Mallat and A. Baiker, *Chem.–Eur. J.*, 2010, **16**, 2181; (*d*) J. Keilitz, S. Nowag, J.-D. Marty and R. Haag, *Adv. Synth. Catal.*, 2010, **352**, 1503; (*e*) F. Hoxha, E. Schmidt, T. Mallat, B. Schimmoeller, S. E. Pratsinis and A. Baiker, *J. Catal.*, 2011, **278**, 94; (*f*) Y. Huang, S. Xu and V. S.-Y. Lin, *ChemCatChem*, 2011, **3**, 690; (*g*) C. Richter, K. V. S. Ranganath and F. Glorius, *Adv. Synth. Catal.*, 2012, **354**, 377; (*h*) F. Kirby, C. Moreno-Marrodan, Z. Baan, B. F. Bleeker, P. Barbaro, P. H. Berben and P. T. Witte, *ChemCatChem*, 2014, **6**, 2904; (*i*) Z. Guan, S. Lu and C. Li, *J. Catal.*, 2014, **311**, 1; (*j*) T. T. Si Bui, Y. Kim, S. Kim and H. Lee, *RSC Adv.*, 2015, **5**, 75272; (*k*) T. S. B. Trung, Y. Kim, S. Kang, S. Kim and H. Lee, *Appl. Catal., A*, 2015, **505**, 319.

14 (*a*) D. Ferri and T. Bürgi, *J. Am. Chem. Soc.*, 2001, **123**, 12074; (*b*) D. Ferri, T. Bürgi and A. Baiker, *Chem. Commun.*, 2001, 1172; (*c*) D. Ferri, T. Bürgi and A. Baiker, *J. Catal.*, 2002, **210**, 160; (*d*) A. Kraynov, A. Suchopar, L. D'Souza and R. Richards, *Phys. Chem. Chem. Phys.*, 2006, **8**, 1321; (*e*) A. Vargas and A. Baiker, *J. Catal.*, 2006, **239**, 220.

15 Only platinum nanoparticles immobilised in imidazolium-based ionic liquids in the presence of cinchonidine were previously applied in enantioselective hydrogenations: M. J. Beier, J.-M. Andanson, T. Mallat, F. Krumeich and A. Baiker, *ACS Catal.*, 2012, **2**, 337.

16 T. Kusukawa, G. Niwa, T. Sasaki, R. Oosawa, W. Himeno and M. Kato, *Bull. Chem. Soc. Jpn.*, 2013, **86**, 351.

17 For a representative example, see: M. Gómez, K. Philippot, V. Collière, P. Lecante, G. Muller and B. Chaudret, *New J. Chem.*, 2003, **27**, 114.

18 For a selected work, see: H. I. Lee, S. H. Joo, J. H. Kim, D. J. You, J. M. Kim, J.-N. Park, H. Chang and C. Pak, *J. Mater. Chem.*, 2009, **19**, 5934.

19 Commercially available cinchonidine (**a**) and quinidine (**d**) contain less than 8% of the corresponding hydro-alkaloid (**a**/**aH** = 24/1 (4% **aH**); **d**/**dH** = 12/1 (8% **dH**), see Fig. S7 in the ESI†).

20 I. Favier, P. Lavedan, S. Massou, E. Teuma, K. Philippot, B. Chaudret and M. Gómez, *Top. Catal.*, 2013, **56**, 1253.

21 The diameter of MNPs considering a compact packing (for PdNPs, fcc structure) gives the number of layers and in consequence the total number of metal atoms in the nanocluster. Then for **PdIa** with a mean diameter of 2.1 nm, the nanoclusters are constituted by 4 shells of Pd atoms leading to 309 atoms per nanoparticle; for **PdId**

(mean diameter of 1.4 nm), each nanoparticle is constituted by 3 shells, then 147 atoms per nanocluster see G. Schmid, *Chem. Rev.*, 1992, **92**, 1709.

22 A. M. López-Vinaso, I. Favier, C. Pradel, L. Huerta, I. Guerrero-Ríos, E. Teuma, M. Gómez and E. Martin, *Dalton Trans.*, 2014, **43**, 9038.

23 For a contribution concerning the binding energies for N 1s of organic compounds, see: W. J. Gammon, O. Kraft, C. Reilly and B. C. Holloway, *Carbon*, 2003, **41**, 1917.

24 For some selected recent works, see: (*a*) V. V. Zhivonitko, I. V. Skovpin, M. Crespo-Quesada, L. Kiwi-Minsker and I. V. Koptyug, *J. Phys. Chem. C*, 2016, **120**, 4945; (*b*) K.-H. Dostert, C. P. O'Brien, F. Ivars-Barcelo, S. Schauermann and H.-J. Freund, *J. Am. Chem. Soc.*, 2015, **137**, 13496; (*c*) J. Sauer and H.-J. Freund, *Catal. Lett.*, 2015, **145**, 109; (*d*) M. A. Mahmoud, R. Narayanan and M. A. El-Sayed, *Acc. Chem. Res.*, 2013, **46**, 1795.

25 J. Wu, S. Lu, D. Ge and H. Gu, *RSC Adv.*, 2015, **5**, 81395.

26 For some selected contributions, see: (*a*) G. Guillena, D. J. Ramón and M. Yus, *Chem. Rev.*, 2010, **110**, 1611; (*b*) S. Bähn, S. Imm, L. Neubert, M. Zhang, H. Neumann and M. Beller, *ChemCatChem*, 2011, **3**, 1853.

27 For a selected review, see: M. A. Keane, *ChemCatChem*, 2011, **3**, 800.

28 T. Hara, T. Kaneta, K. Mori, T. Mitsudome, T. Mizugaki, K. Ebitani and K. Kaneda, *Green Chem.*, 2007, **9**, 1246.

29 The hydrodehalogenation of 4-bromophenol was carried out at larger scale than that described for the rest of reactions studied in this manuscript: a scale-up of three times, meaning that 3 mL of catalytic solution of **PdId** was used, with the aim of characterising the stabiliser by ^{1}H NMR after catalysis. Conversion and yield were similar to those obtained using 1 mL of catalytic solution (98% conversion and 93% yield). After extraction of phenol, 3 mmol of 1-dodecanethiol were added to the glycerol catalytic phase under argon and stirring for 24 h, with the aim of removing the stabiliser from the metal surface. Extraction with dichloromethane from the glycerol phase permitted to recover the ligand as a mixture of quinidine (**d**) and hydroquinidine (**dH**), in a ratio 70/30 respectively (see Fig. S20†), analogously to that obtained after the synthesis of **PdId** (see above in the section Synthesis and characterisation of palladium nanoparticles).

